Direct piezoelectric effect in geopolymeric mortars

Caterina Lamuta[a], *Sebastiano Candamano*[b], *Fortunato Crea*[b], *Leonardo Pagnotta*[a]*

[a] University of Calabria, Department of Mechanical, Energy and Management Engineering – DIMEG, Ponte P. Bucci, cubo 44C, 87030 Arcavacata di Rende (CS)

[b] University of Calabria, Department of Environmental and Chemical Engineering – DIATIC, Ponte P. Bucci, cubo 44A, 87030 Arcavacata di Rende (CS)

*corresponding author, e-mail: leonardo.pagnotta @unical.it

Abstract

In this paper the occurrence of a direct piezoelectric effect has been discovered for the first time in a metakaolin based geopolymeric mortar. Unlike any other known piezoelectric material (quartz single-crystal, PZT, PVDF), wherein the formation of local electric dipoles is due to the elastic deformation of the non-centrosymmetric crystalline structures, a new and different piezoelectric mechanism was observed in geopolymers. It is due to a complex interplay that involves not-framework cations, framework and water contained in the material pores. In particular, the model proposed by authors attributes the piezoelectric effect to the charge imbalance and local dipoles generated under compressive stress by the migration, within the network of interconnected pores of geopolymer, of the hydrated Na^+ cations, coordinated in a charge balancing arrangement with the aluminum tetrahedra. The absence of a charge generation in dehydrated samples and the inexistence of a converse piezoelectric response confirmed that quartz impurities present inside the material don't contribute to the direct piezoelectric effect, thus due only to ionic mobility. Furthermore, an anisotropic behavior of the effect was observed and the measured charge coefficient in

the predominant direction was found to lie in the range (4÷40) pC/N, depending on the water content in geopolymers.

Keywords: geopolymers, direct piezoelectric effect, ionic mobility, anisotropy

1. Introduction

To date an increasingly number of smart materials have been designed, developed and applied in a variety of biomedical and electromechanical devices. Among them, piezoelectric materials have received great attention due to their technological impact. The most common used piezoelectric materials are lead zirconate titanate, a piezoelectric ceramic, or piezoceramic known as PZT [1,2] and piezoelectric polymers based on poly(vinylidene fluoride) [3]. PZT piezoelectric effect is due to the elastic deformation of its non-centrosymmetric crystalline structure, while in PVDF it is due to its molecular structure and orientation [4]. Natural piezoelectric materials also exist and include tourmaline, quartz, topaz, cane sugar and Rochelle salt. Hardened cement pastes have also shown a stress dependent voltage ascribable to the electrical double layer peculiar of their microstructure [5,6,7]. To the knowledge of the authors, no works have been focused on studying the piezoelectric properties of geopolymers.

Geopolymers are recent developed ceramic materials produced by alkaline activation of thermally activated natural materials like metakaolin [8]. These sources are dissolved in an alkaline activating solution and subsequently polymerize into a network thus hardening at low or room temperatures. Geopolymers show very interesting properties, whether used pure, with fillers or reinforced [9]. They can find applications in many fields such as in the civil engineering, as fireproof building materials, in automotive and

aerospace industries, non-ferrous foundries and metallurgy, ceramics and plastics industries, radioactive and toxic waste management, art and decoration etc [10, 11, 12, 13]. Many studies have been carried out on their structural characterization, on the investigation of geopolymerization mechanism, on how the raw material selection and processing conditions affect their fresh state, microstructure, chemical and mechanical behaviour [14, 15, 16, 17].

In this paper we show, for the first time, that geopolymers present a direct piezoelectric effect, by proposing a physical-chemical model for the explanation of the observed phenomenon. The discovery of the piezoelectric activity in geopolymers, low cost and eco-friendly materials [14], paves the way for several interesting applications, e.g. sensors, transducers, self-monitoring of civil infrastructures or energy harvesting [18].

2. Materials and Methods

2.1 Materials

Metakaolin having a D10 of 0.51 μm, a D50 of 1.59 μm and a D90 of 9.74 μm, based on a volume distribution, was provided by Doldes Massara S.r.l. Sodium silicate solution was provided by Condea Augusta S.P.A. The weight composition of metakaolin , as determined by X-ray fluorescence, is: Al_2O_3 (42 %), SiO_2 (53.2 %), K_2O (0.3 %), Na_2O (0.1 %), Fe_2O_3 (1.5 %), TiO_2 (1.9 %), Loss of Ignition at 995°C (1.0 %). The weight composition of sodium silicate solution is: SiO_2 (29.5 %), Na_2O (13.8 %), H_2O (56.7 %). Silica sand passing 500 μm was used as filler. Deionized water was used throughout the experiments to avoid the effects of unknown contaminants in water. Na(OH) 99.9% pure was purchased by Sigma-Aldrich.

PZT piezoceramic samples (PIC181, hard) were purchased by Physik Instrumente (PI) for the measurement setup verification.

2.2 Geopolymer synthesis and curing

Geopolymers were synthesized by activating metakaolin with the alkaline silicate solution [8]. In order to guarantee good mass transfer and dissolution rate, the maximum extent of metakaolin reaction and aluminium incorporation in geopolymer matrix, the following molar ratios SiO_2/Na_2O=1.62 and H_2O/Na_2O=12.25 have been used to prepare the alkaline silicate solution. Firstly, the sodium hydroxide solution was obtained by dissolution of NaOH pellets in ultrapure water, with container kept sealed wherever possible to minimize contamination by atmospheric carbonation and prevent water evaporation. The solution was stirred until the NaOH pellets had dissolved and the solution became clear. Once cooled down it was poured into sodium silicate solution. The so obtained alkali activator solution was covered, sealed, stirred and allowed to cool back down to room temperature. Finally, the activator solution was added to metakaolin powder and the slurry was mechanically vigorously mixed for 10 minutes. The last step involved sand addition and mechanically mixing for 5 min. The slurries were, afterwards, rapidly casted into open and dismountable Teflon moulds in order to obtain cubic samples of dimensions 20 mm × 20 mm × 20 mm.

All samples were placed on the vibration table to remove entrained air. In order to prevent the moisture loss, the moulds were sealed from the atmosphere and cured for 24 h at 50°C. The sealed specimens were then stored at ambient temperature and pressure for four weeks to complete curing.

The final theoretical composition of geopolymers, in terms of oxides, is equal to Na_2O-

$3.86SiO_2$-Al_2O_3-$5.22H_2O$. Al/Na molar ratio was fixed equal to one because sodium balances the negative framework charge carried by tetrahedral aluminium, thus acting as structure forming agent. SiO_2/Al_2O_3 molar ratio was fixed to 3.86 in order to minimize geopolymer porosity thus increasing mechanical performance [19]. The Water/Binder (W/B) weight ratio was fixed at 0.56 to obtain a good mortar workability. Sand/Binder (S/B)=1.5 has been used to prevent microcracks due to shrinkage.

In order to check data repeatability, four batches of five specimens each were realized and tested.

2.3 Chemical characterization

Phase identification of prepared geopolymeric pastes was carried out recording X-Ray diffractograms, using CuKα radiation in 2θ = 5°- 50° range (Philips PW 1730/10 generator equipped with a PW 1050/70 vertical goniometer, λ = 1.5404 Å), with step of 0.02° and a scan rate of 1°/min

Thermogravimetric analysis was performed on a Netzsch STA 409 analyzer, at a heating rate of 10°C/min in air from 20°C to 820°C. ^{29}Si MAS-NMR, ^{27}Al MAS-NMR and ^{23}Na MAS-NMR analysis were performed on a Bruker 600 spectrometer. For ^{29}Si (119.2 MHz), at 3 μs (θ = π/4) pulse was used with a repetition time of 30 s, for ^{27}Al (156.37 MHz), at 2 μs (θ = π/4) pulse was used with a repetition time of 1 s, for ^{23}Na (158.74 MHz), at 4 μs (θ = π/4) pulse was used with a repetition time of 1 s.

N_2 adsorption/desorption plots of powdered geopolymer paste were carried out in micromeritics ASAP 2020 instruments. Before the analysis, all samples were pretreated in vacuum condition at 200° C for 12 h. The specific surface area was calculated using the Brunauer–Emmet–Teller method. Mesopore diameter distributions was determined

with the Barret–Joyner–Halenda (BJH) method using the desorption data.

2.4 Direct piezoelectric characterization

The direct piezoelectric characterization was carried out by means of a quasi-static method [20]. Schematic representation of the setup realized for the direct piezoelectric characterization with the adopted reference system, referred to the casting process, is reported in Figure 1. The mechanical input was imposed by means of an electro-mechanical Instron biaxial testing machine (ElectroPlus E10000) provided with a 10 kN load cell. Samples were tested under cycling compression load with a static pre-load of 1.25 kN and a frequency of 3 Hz. A light dependence of the charge coefficient from pre-load and frequency was observed and the chosen values of 1.25 kN and 3 Hz are those for which the higher coefficient was measured. The steel loading plates were electrically isolated by means of mika foils 300 μm thick and two copper foils, with the same dimensions of the sample surface and 200 μm thick, were used as electrodes. An HBM digital charge amplifier (CMD600), with a measuring range of 50-600000 pC, was used to measure the produced electric charge and a HBM Universal DAQ amplifier (QuantumX MX 840B) to real-time data recording. The HBM software catmanEasy-AP was used for data acquisition. After the acquisition of the sinusoidal signal of both of the applied load and the produced electric charge, the charge coefficient, d_{ii} (where i varies from 1 to 3, depending on the analyzed direction, according to the adopted reference system), was obtained as the ratio between the charge and the load amplitude. In particular, the charge amplitude was measured after the stabilization of the charge signal. In Figure 1 raw data referred to a test performed with a load amplitude of 250 N are reported.

The reliability of the measuring system was verified by testing commercial PZT piezoelectric ceramic materials of known charge coefficients, characterized by means of standard dynamic procedures [21] by the supplier company. The quasi-static characterization with the realized setup led to the same values of the charge coefficient declared by the supplier (as shown in "Supplementary Information" documentation), with the advantage that, compared to standard procedures, it is easier to implement. Contrary to dynamic procedures in fact it doesn't need of a particular sample geometry (that must be such that only a pure fundamental resonance mode is produced) and a high frequency (in the range of the resonance response).

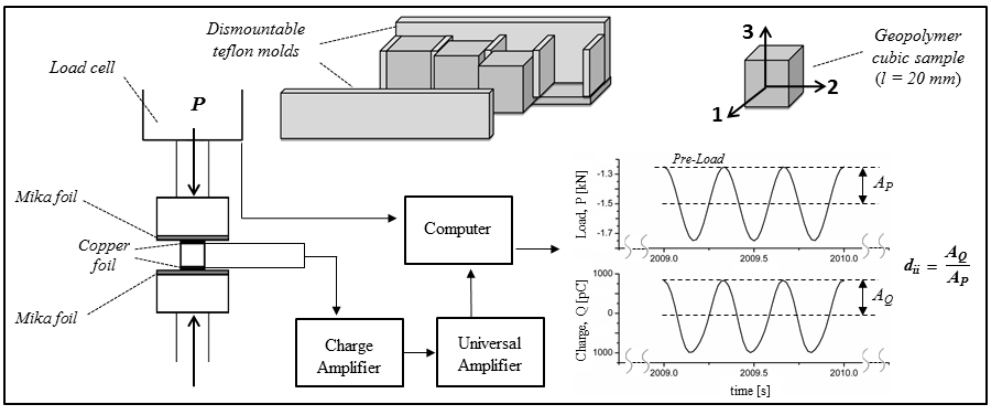

Figure 1. Schematic representation of the setup realized for the direct piezoelectric characterization with the adopted reference system.

2.5 Converse piezoelectric characterization

For the converse piezoelectric characterization samples were electrically excited with an AC voltage of 10 V amplitude at frequencies ranging from 50 mHz to 10 Mz by means of a function generator (HAMEG HM8030-6). Samples were clamped with a pre-load of 1.25 kN and electrically isolated by means of mika foils, whereas copper foils were used as electrodes. The output strain was measured by means of stain gauges

glued on samples and a HBM strain gauge bridge amplifier (QuantumX MX 1615), with the catmanEasy-AP software, was used to real-time data recording.

3 Results and Discussion

Figure 2 shows results about the direct piezoelectric characterization along direction 3.

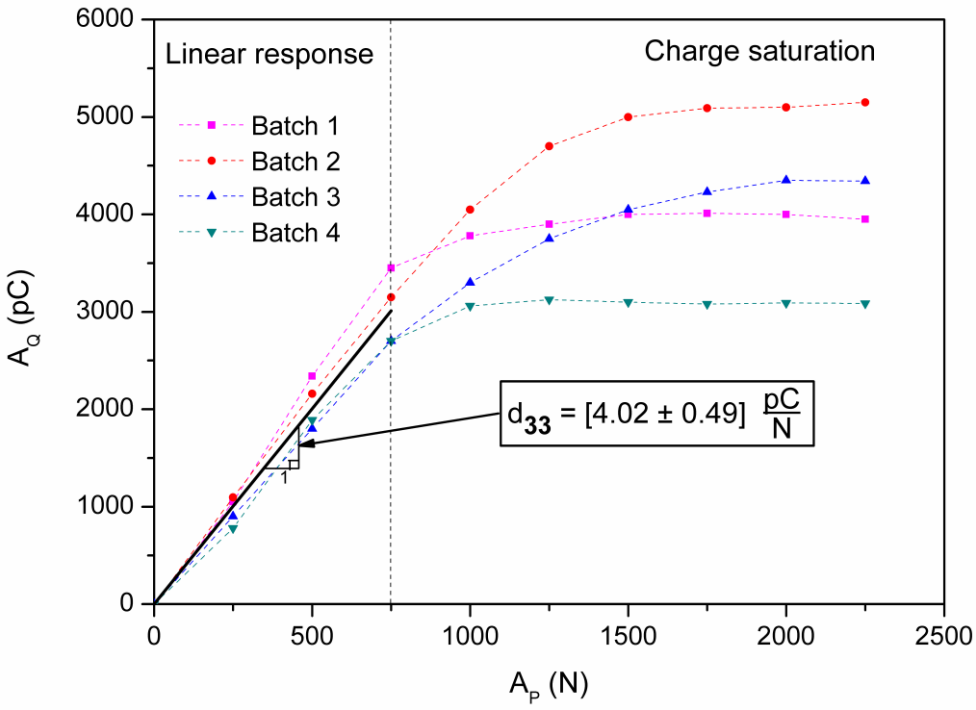

Figure 2. Charge amplitude A_Q versus load amplitude A_P for four batches of five samples tested along direction 3, which is that normal to mold's open surface. The continuous black line represents the average curve in the linear region whose slope represents the charge coefficient d_{33}.

In particular, four batches of five specimens were tested with different load amplitude values. In Figure 2 the different curves refer to different batches whereas each point of the curve represents the average value of the five samples of each batch.

It is worth noting that the material exhibits an initial linear behavior followed by a stabilization to a plateau value, associated to charge saturation. The continuous black line in Figure 2 represents the average curve in the linear region whose slope represents the charge coefficient d_{33}, equal to (4.02 ± 0.49) pC/N. Experimental data about the

mechanical or electromechanical characterization of ceramic materials are usually quite scattered because of the randomly porous nature of such materials and the standard deviation value of the charge coefficient measured for geopolymers is low enough to highlight the good repeatability of the carried out measurements.

Also d_{11} e d_{22} were determined, but, since the piezoelectric activity along directions 1 and 2 was found to be really weak, their values are negligible because they can be confused with the experimental noise. Such results highlight then the presence of an anisotropic behavior of the piezoelectric effect in geopolymers.

Since piezoelectricity is related to the generation of electrical dipoles within the material microstructure, several analysis were carried out by authors on the produced geopolymer mortar in order to understand the observed phenomena and to propose a chemical-physical model able to explain the piezoelectric mechanism in such a material. Even if geopolymers are X-ray amorphous, XRD analysis is usually carried out to check the presence of any undesired crystalline phases developed during curing that could affect mechanical properties, such as zeolites, or already present in the parent materials as impurities, like quartz or crystalline kaolinite. In particular, these last, having a non-centrosymmetric structure could contribute to the generation of electrical dipoles during mechanical stress [18]. Figure 3 (a) shows the XRD patterns of metakaolin raw powder (lower curve) as well as that of the synthesized geopolymer (upper curve). Metakaolin exhibits a pronounced broad hump centered at approximately 22° 2θ with few peaks, indicating that it contains essentially amorphous silica and alumina and Quartz (PDF n° 01-083-2468) and Muscovite (PDF n° 00-002-0055) impurities as crystalline phases. No diffraction peaks of its parent material, kaolinite, were detected. After reaction with sodium silicate solution, XRD pattern shows a shift of the centre of the original broad

hump from 22° 2θ to approximately 28° 2θ, that can be considered the typical distinguishing feature of the geopolymeric materials [14]. All sharp peaks from crystalline phase in parent material are still present in the geopolymer diffraction pattern, thus confirming that they behave as inactive fillers in the geopolymer binder. Quartz could indeed contribute, even if unlikely to occur, since the crystal need to be cut and loaded along its symmetry directions [22], to the generation of electrical dipoles during mechanical stress, thus to piezoelectric activity. The obtained geopolymers show a dense and homogeneous microstructure, as revealed by SEM analysis shown in Figure 3 (c), that conventionally is considered as a strong indicator of high strength.

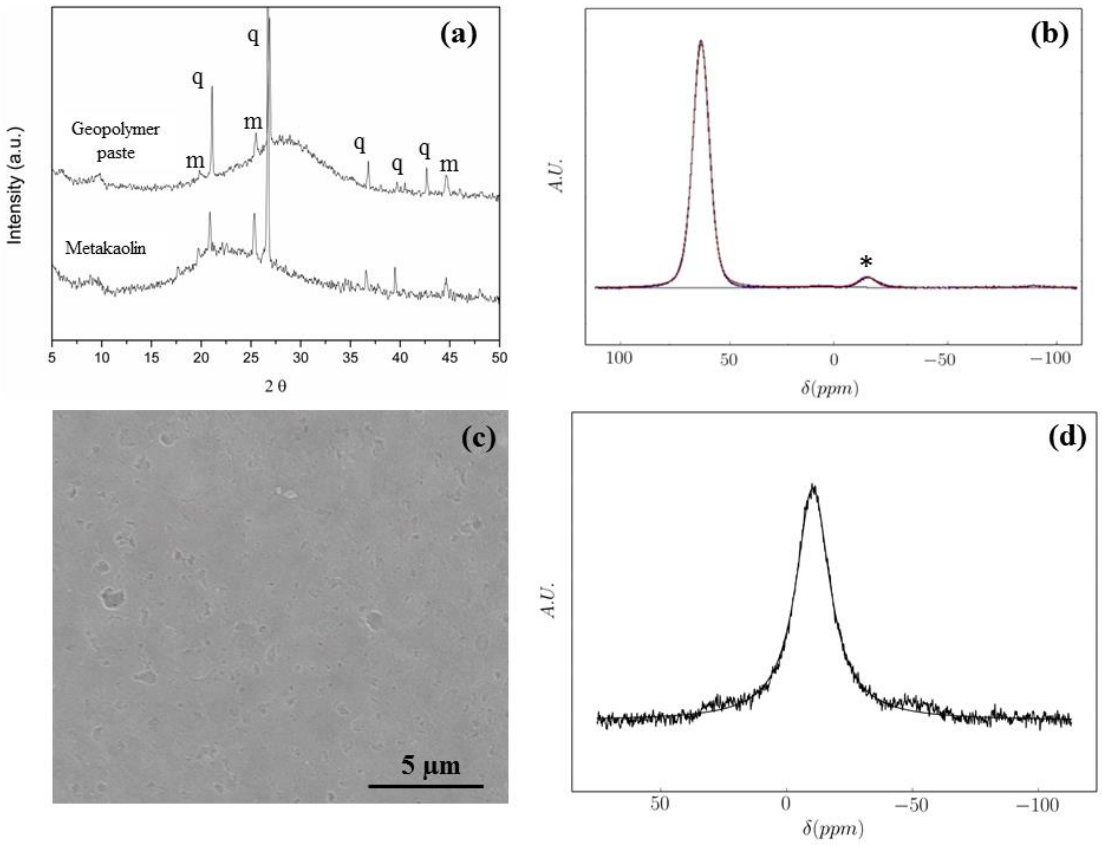

Figure 3. a) XRD patterns of metakaolin and geopolymer pastes (q= quartz, m= muscovite); b) ^{27}Al-NMR, c) SEM of geopolymer mortar d) ^{23}Na-NMR of geopolymer paste. The symbol * denotes spinning sidebands

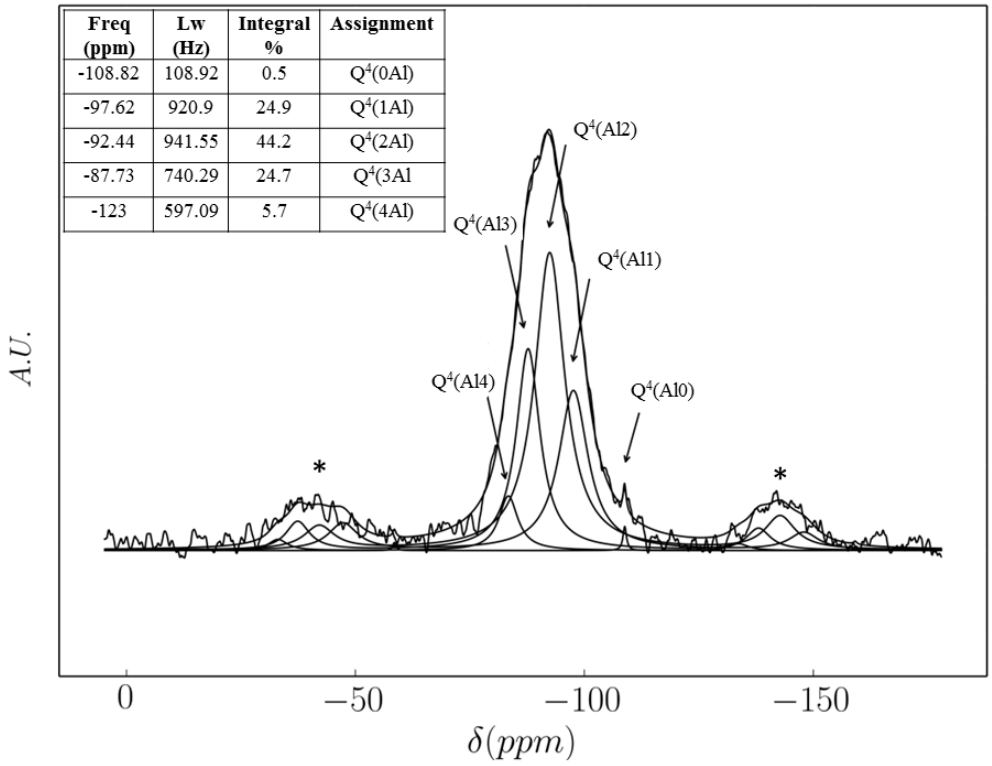

Figure 4. ^{29}Si-NMR of geopolymer paste

In order understand the structural properties and the formation process of the produced geopolymer and detect a possible generation of electric charge imbalance, solid state ^{29}Si- MAS-NMR, ^{27}Al- MAS-NMR and ^{23}Na- MAS-NMR analyses were carried out.

Geopolymers can be generally described as a three dimensional amorphous network built from TO_4 (T=Si,Al) tetrahedral, joined at the corners with oxygen. The single negative charge associated with aluminium (III) in tetrahedral co-ordination is usually balanced by extraframework cations present in framework cavities [23]. Furthermore, recent papers have regarded them as amorphous analogues of zeolites [23,24], because the presence of deformed six-, eight- and ten-membered rings results in the possibility of replacing the extra-framework cations by ion exchange [25].

^{29}Si- MAS-NMR is used to differentiate the connectivity range of SiO_4 tetrahedra and

in the determination of substitution of Al for Si tetrahedra. ^{29}Si MAS-NMR decomposed spectrum of geopolymer gel, as reported in Figure 4, exhibits a broad spectrum, indicative of short-range ordering, centered at -94 ppm, reflecting the incorporation of Al into the coordination sphere of the Si and comprising all five possible silicon Q^4(mAl) species. The consistency of the decomposition has been assessed with respect to the nominal composition of geopolymer [26].

^{27}Al- MAS-NMR spectrum of geopolymer, shown in Figure 3 (b), provides additional and important structural informations, because peaks related to the various coordinations of oxygen around Al atoms are clearly defined. It exhibits a dominant line at 63 ppm due to tetrahedral aluminum sites, as expected for a true geopolymer [27]. The absence of the resonance line at 28 ppm due to Al(V) clearly shows that almost all Al(V) contained in metakaolin is consumed during the geopolymerization process. The really weak ^{27}Al- MAS-NMR line at about 8 ppm is due to the presence of octahedral Al(VI) aluminum sites and their amount (0.46%) can be attributed to negligible amount of unreacted metakaolin.

The ^{23}Na-NMR spectrum of geopolymer, shown in Figure 3 (d), exhibits a signal at –10 ppm, that is associated with the presence of partially hydrated cation Na^+, coordinated with the aluminium replacing the silicon in a charge balancing arrangement.

The detected presence of the partially hydrated cation Na^+ in charge balancing arrangement is a key factor for the piezoelectric effect explanation in geopolymers. In fact hydration reduces the cation–lattice electrostatic interaction through cation–water interaction, thus resulting in a weaker bonding that promotes the Na^+ migration away from the framework wall during mechanical loading and therefore creates the charge imbalance. Analogue mobility of non-framework cations, by hydrating at ambient

conditions or under pressure, in presence of water has been widely studied in zeolite [28,29,30].

The presence of water inside of the geopolymer structure is therefore another key factor for explaining the observed piezoelectricity and it has been measured through thermogravimetric analysis. The mass loss (TG) and derivative mass loss (DTG) curve are reported in Figure 5 (a). The weight loss, of about 8%, has two maximum rates around 50 °C and 100 °C and it is completed at 200 °C. It is associated to the dewatering process and it can be attributed to the removal of free water in the pores (up to ≈100 °C) or physically adsorbed water, e.g. capillary encapsulated water up to ≈200 °C. A residual of 91% remained at 820 °C. The thermogravimetric analysis showed than that water is present in geopolymer pores. In order to study the textural properties and the pores morphology of geopolymer paste, N_2 adsorption-desorption isotherms was carried out and results are reported in Figure 5 (b). The geopolymer paste shows a type IV isotherm with a H3 hysteresis loop characteristic of slit-shaped mesoporous structure. The specific surface area, with a value equal to 34.2 m^2/g, was calculated using the Brunauer–Emmet–Teller (BET) method. The total pore volume equal to 0.1888 cm^3/g was derived from the amount of vapor adsorbed at a relative pressure close to unity. Mesopore width distributions was determined with the Barret–Joyner–Halenda (BJH) method using the desorption data. The pore size distribution of the specimen, reported in Figure 5 (c), is observed to be bimodal. It can be explained as a consequence of the pores interconnectivity and it is expected to favor water mobility under the mechanical loading.

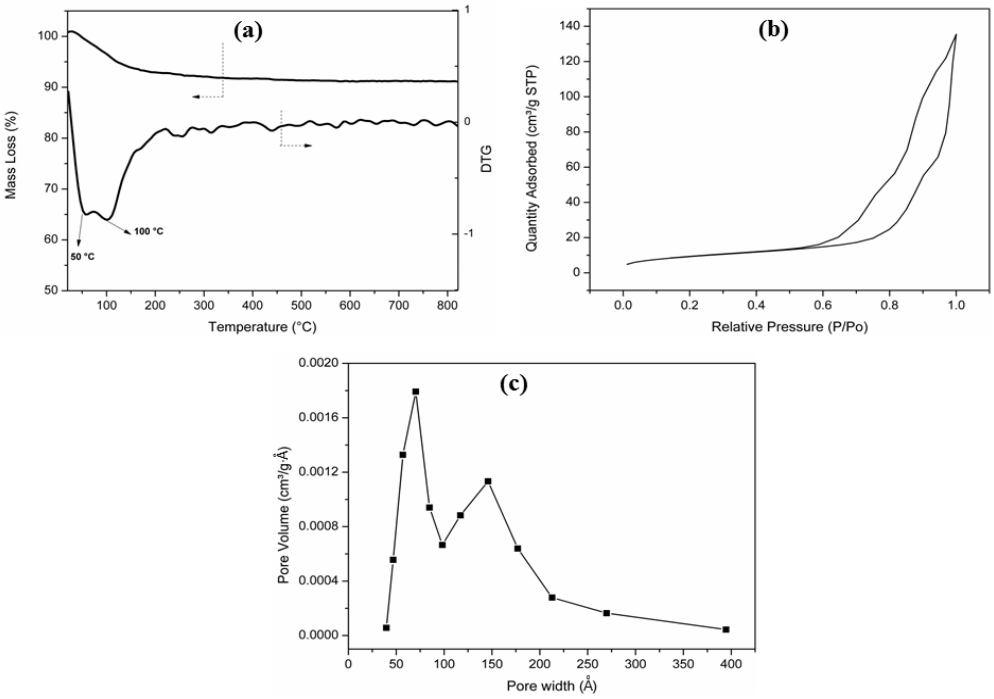

Figure 5. a) Thermogravimetric data of geopolymer paste: mass loss and mass loss derivative (DTG) curves; b) N_2 Isotherms of geopolymers paste; c) Pore width distribution (BJH desorption) of geopolymer paste.

On the bases of results of microstructural and chemical characterizations reported above one can propose a plausible model (schematically shown in Figure 6) able to explain the detected direct piezoelectric effect in geopolymers. It arises from its dense and homogeneous microstructure with a distributed and interconnected slit-shaped mesoporous porosity which embeds evaporable free or physically adsorbed water and extraframework, mobile, hydrated alkali Na^+ cations. Piezolectric effect is thus promoted by the migration of mobile hydrated cations under compressive loading in the pores of the geopolymeric matrix, thus creating a charge imbalance and local dipoles. The mechanism is coherent with the one proposed for explaining the piezoelectric effect in cement pastes [7, 31]. Similarities occur in the elements that determine and control the observed phenomenon, i.e. the presence of porosity, water and the transportation of mobile ions. What differs is the nature and the origin of ions. In Portland cement, the

main hydration product is C–S–H. It is in contact with a high pH electrolyte solution, containing $Ca(OH)_2$ (Portlandite), that promotes the dissociation of its surface silanol group (SiOH) and the successive physical adsorption of mobile calcium ions. The mechanism of surface charge creation (Electric Double Layer) is thus responsible of the charge imbalance and local dipoles under mechanical loading. In the case of geopolymers, instead, as evidenced by all the analysis carried out, it is due to the presence of the non-framework and hydrated Na^+ cations that balance the single negative charge associated with aluminium (III) in tetrahedral co-ordination.

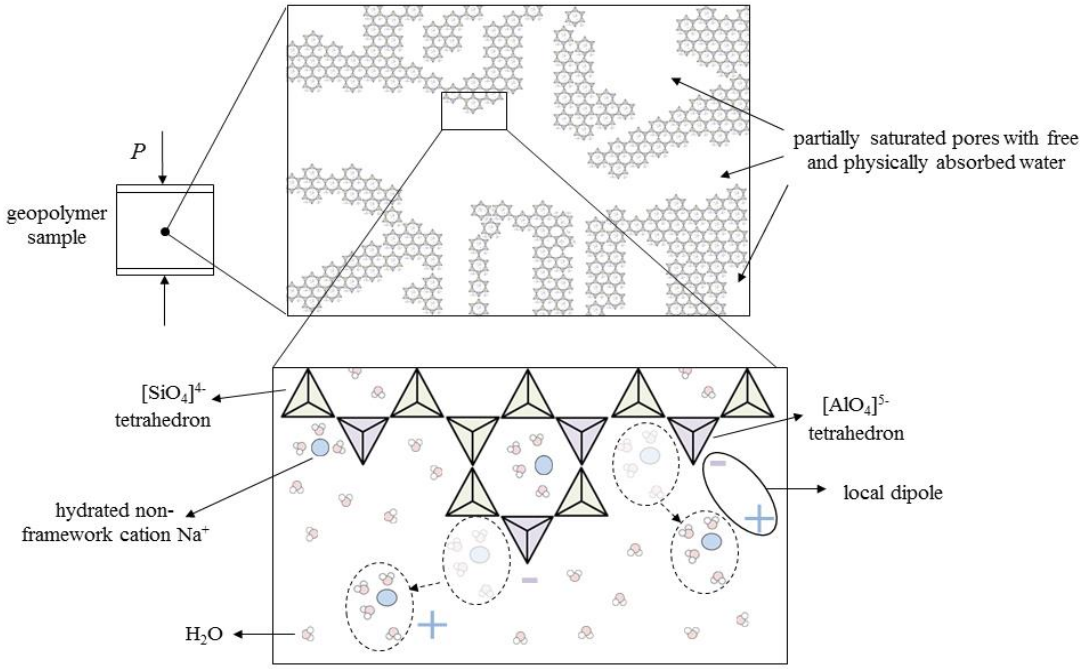

Figure 6. Schematic representation of the chemical-physical model proposed for the explanation of the direct piezoelectric effect detected in geopolymers. The lower magnification represents the porous structure of the material, characterized by partially saturated pores, filled with free and physically absorbed water. The higher magnification shows the amorphous network built from SiO_4 and AlO_4^- tetrahedrons, joined at the corners with oxygen. The single negative charge associated with aluminium (III) in tetrahedral co-ordination is balanced by the non-framework and hydrated Na^+ cations. The sample loading causes a distancing between cations and framework (indicated by dashed circles), fostered by hydration that reduces the cation–lattice electrostatic interaction. This distancing causes a charge imbalance and the formation of local dipoles which represent the cause of the piezoelectric effect.

The piezoelectric model proposed by the authors is thus mainly based on the ionic mobility phenomenon fostered by the water presence. In order to confirm such model and exclude the presence of other phenomena that could contribute to the electric charge generation during mechanical loading as, for example, the elastic deformation of quartz, some specimens were dried in oven under 50 °C until no weight decrease was measured. This thermal treatment allows to greatly decrease the water content without altering the geopolymer structure. During dehydration of geopolymer, pores undergo to a shrinkage process, while Na^+ cations and framework generate strong electrostatic interactions as a consequence of the reduced dielectric screening of water, thus inhibiting cations migration [32, 33] .

It was observed that a completely dried sample (weight increment of 0 % in Figure 7) doesn't exhibit any direct piezoelectric effect, thus excluding any other source of piezoelectricity and confirming the validity of the ionic mobility based model proposed by the authors. Subsequently, the samples were stored under controlled humidity environment, thus allowing them to re-absorb water and the charge coefficients were measured for different water contents. From Fig. 6, it can be observed that the charge coefficient in the predominant piezoelectric direction, d_{33} (black square symbols), increases for increasing values of water content (values more than 40 pC/N were measured in conditions of high hydration, not reported in Figure 6).

An converse piezoelectric characterization was also carried out on the geopolymeric samples. They were electrically excited with an external AC voltage signal in a broad frequency spectrum, but any strain was measured by strain gauges glued on samples, thus confirming that any potentially non-centrosymmetric structures, in particular quartz, contribute to the direct piezoelectric effect.

In Figure 7 it can also observed that, as previously stated, the direct piezoelectric effect in geopolymers is anisotropic. In particular, the direction perpendicular to the mold's open surface, defined as direction 3 in Figure 1, is that along with the higher piezoelectric activity was measured, whereas along directions 1 and 2 the effect is almost negligible and becomes to be influent for high water contents.

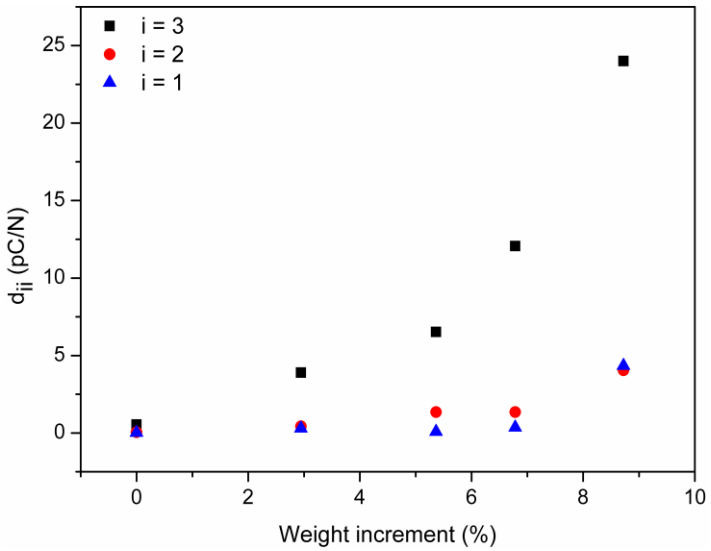

Figure 7. Charge coefficients measured for different water contents along three different directions.

The observed anisotropy with respect to the piezoelectric effect in geopolymer mortar can be ascribed to its porous nature. Anisotropic behaviors, in fact, are generally found and extensively studied in natural porous argillaceous materials (rocks) [34, 35], due the preferential orientation of clay platelets during sedimentation [36]. Several authors (von Engelhardt & Gaida, 1963; Meade, 1964) have also reported that compaction increases that preferential orientation. Direct consequence of this preferred orientation is an anisotropy of tortuosity, that along with constrictivity can generate an anisotropy of effective diffusion and its variation by several factors by varying the direction [37]. As evidenced by scanning electron microscope analysis (SEM, FEI model Inspect) reported in Figure 8, metakaolin, the parent material used to produce geopolymer

mortars, also presents a layered microstructure with particles dominantly plate in shape. Morover, N_2 adsorption-desorption isotherms (Figure 4 (b)) show that the geopolymer paste presents a type IV isotherm with a H3 hysteresis loop characteristic of slit-shaped mesoporous structure, thus confirming a pore structure that arises from parent clay platelets layered structure.

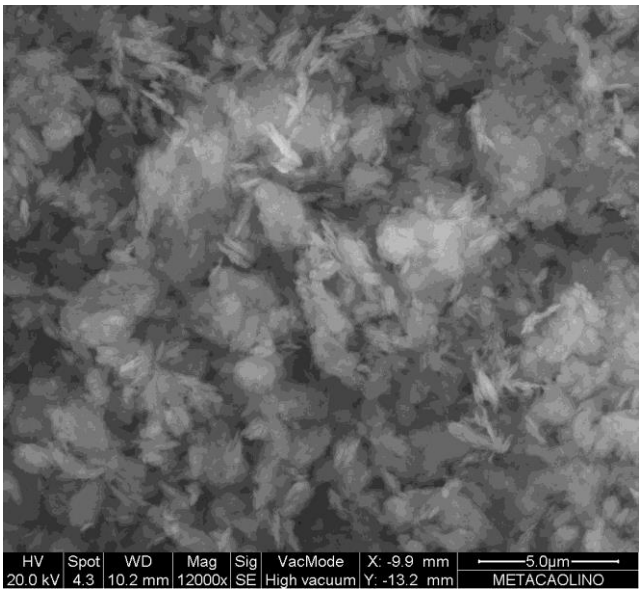

Figure 8. SEM analysis of Metakaolin,

Furthermore recent research works have focused their attention to the contribution of poroelastic behavior to the mechanical properties of cementitious mortars and concrete [38, 39, 40] and to their anisotropic behaviors [41, 42], because porosity structure deeply influences fluid motion and the character and intensity of interactions between fluid and skeleton [36]. The variables that influence the anisotropy in piezoelectric effect measured in geopolymers stem, therefore, from several phenomena, such as direction of casting, curing conditions, water/binder ratio, volume fraction, geometry, dimensions and interconnections of the pores, degree of saturation and preferential

orientation of metakaolin platelets. Due to the complexity of the involved phenomena, further investigations are necessary to develop a deterministic model.

In this paper authors attributed the observed electromechanical coupling to a direct piezoelectric effect. However the electromechanical coupling is not only related to piezoelectricity. It could indeed occur through different mechanisms such as electrostriction, flexoelectricity and Maxwell stress.

Concerning electrostriction and Maxwell stress effect, related to the strain produced by the application of an external electric field, because it was verified that the application of an external electrical field doesn't produce any strain in geopolymers, such material can't present these properties.

About flexoelectricity, it occurs in liquid crystals or in solids with a crystal symmetry and it is defined as the polarization produced by a strain gradient. This strain gradient is generally produced by bending stress. In this work geopolymers were tested by means of compression tests that produce a homogeneous strain on the material, therefore the electromechanical coupling can't be related to flexoelectricity because any strain gradient was imposed on the tested samples.

For these reasons authors attributed the observed electromechanical coupling to a direct piezoelectric effect.

4 Conclusions

The presence of a direct piezoelectric effect has been discovered for the first time in a metakaolin based geopolymeric mortar and a chemical-physical model for the explanation of the observed phenomenon is proposed in this paper.

In particular, this model ascribes the piezoelectric effect to the charge imbalance and local dipoles generated under compressive stress by the migration, within the network

of interconnected pores of geopolymer, of the hydrated Na^+ cations, coordinated in a charge balancing arrangement with the aluminum tetrahedra. The absence of a charge generation in dehydrated samples and the inexistence of a converse piezoelectric response confirmed the validity of the proposed model by demonstrating that piezoelectricity is not necessarily related to the deformation of a non-centrosymmetric structure.

Furthermore, an anisotropic behavior of the effect, related to the porous structure of the material, was observed and the measured charge coefficient in the prevalent direction was found to lie in the range (4÷40) pC/N, depending on the water content in geopolymers.

The discovery of the piezoelectric activity in geopolymers paves the way for several interesting applications. Due to its promising application in the field of structural components, geopolymer can allow the real time self-monitoring of civil infrastructures. The use of such a material could eliminate or reduce the need for embedded or attached devices, which are expensive, limited in durability and, as in the case of lead zirconate titanate, have negative environmental impact due to the presence of lead. Furthermore, they have low cost production and components of various shapes and dimensions can be easily fabricated. Geopolymers indeed do not need to be cut along particular directions like quartz crystals, neither to be polarized like piezoceramics or piezopolymers materials.

Acknowledgements

The authors wish to thank the Laboratory of Nuclear Magnetic Resonance of Trisaia ENEA Research Centre for performing NMR measurements.

The authors acknowledge funding from PON MaTeRiA (Grant No. PONa3_00370).

References:

[1] Tingting Xu, Chang-An Wang, Control of pore size and wall thickness of 3-1 type porous PZT ceramics during freeze-casting process, Materials and Design, 2016, 91, 242–247

[2] C.H. Zhang , Z. Hu , G. Gao , S. Zhao , Y.D. Huang, Damping behavior and acoustic performance of polyurethane/lead zirconate titanate ceramic composites, Materials and Design, 2013, 46, 503–510

[3] J. Nunes-Pereira , P. Martins , V.F. Cardoso, C.M. Costa, S. Lanceros-Méndez, A green solvent strategy for the development of piezoelectric poly(vinylidene fluoride–trifluoroethylene) films for sensors and actuators applications, Materials and Design, 2016, 104, 183–189

[4] Khaled S Ramadan, D Sameoto, S Evoy, A review of piezoelectric polymers as functional materials for electromechanical transducers, Smart Mater. Struct., 2014, 23 033001

[5] F.H Wittmann, Observation of an electromechanical effect of hardened cement paste Cem. Concr. Res., 3 (1973), pp. 601–605

[6] M Sun, Q Liu, Z Li, Y Hu, A study of piezoelectric properties of carbon fiber reinforced concrete and plain paste during dynamic loading, Cem. Concr. Res., 2000, 30 (10), pp. 1593–1595

[7] Mingqing Sun, Zhuoqiu Li, Xianhui Song, Piezoelectric effect of hardened cement paste, Cement and Concrete Composites, 2004, 26 (6), 717–720

[8] J. Davidovits, Geopolymer Chemistry and Application (3rd ed.) Institute Geopolymer, Saint Quentin, France 2008.

[9] T. Alomayri, F.U.A. Shaikh, I.M. Low, Effect of fabric orientation on mechanical properties of cotton fabric reinforced geopolymer composites, Mater Design, 2014, 57, 360-365

[10] W. Yodsudjai, P. Suwanvitaya, W. Pikulprayong, B.Taweesappaiboon, Testing of geopolymer Mortar properties for Use as Repair Material, Design, in Development, and Applications of Engineering Ceramics and Composites: Ceramic Transactions, eds D. Singh, d, Zhu, Y. Zhou, and M. Singh, new York 2010, vol 215

[11] T. Hanzlicekw, M. Steinerova,-Vondrakova, Immobilization of toxic metals in solidified systems of siloxo-sial networks, J. Am. Ceram. Soc. ,2006, Vol 89(3), 968-970.

[12] J. Davidovits, M. Davidovics, Geopolymer: Ultra High Temperature Tooling Material for the Manifacture of Advanced Composite, 1991, Proc. 36th Int'l SAMPE symposium, 1939-1949.

[13] S. Candamano, P. Frontera, A. Macario, F.Crea, J.B. Nagy, P.L.Antonucci, Preparation and characterization of active Ni-supported catalyst for syngas production, Chemical Engineering Research and Design, 96, 2015, DOI: 10.1016/j.cherd.2015.02.

[14] P. Duxson, A. Fernández Jiménez, J. L. Provis, G. C. Lukey, A. Palomo ,J. S. J. van Deventer, Geopolymer technology: the current state of the art**,** J. Mat Science, 2007**,** 42, 2917 – 2933.

[15] Shadi Riahi, Ali Nazari, Davood Zaarei, Gholamrez Khalaj, Hamid Bohlooli, Mohammad Mehdi Kaykha, Compressive strength of ash-based geopolymers at early ages designed by Taguchi method, Mater Design, 2012, 37, 443-449

[16] Ali Bagheri, Ali Nazari, Compressive strength of high strength class C fly ash-based geopolymers with reactive granulated blast furnace slag aggregates designed by Taguchi method, Mater Design, 2014, 54, 483-490

[17] Dongming Yan, Shikun Chen, Qiang Zeng ⁎, Shilang Xu, Hedong Li, Correlating the elastic properties of metakaolin-based geopolymer with its composition, Mater Design, 2016, 95, 306-318

[18] K. Uchino, Advanced Piezoelectric Materials, (Woodhead Publishing, 2010)

[19] P. Duxson, S.W. Mallicoat, G.C. Lukey, W.M. Kriven, J.S.J. van Deventer, Colloids and Surfaces A: Physicochemical and Engineering Aspects, 2007, 292, 8–20.

[20] M. G. Cain, Characterisation of Ferroelectric Bulk Materials and Thin Films, Springer Series in Measurement Science and Technology 2, 2014, pages 37-64.

[21] European standard, EN 50324-2: 2002, Piezoelectric properties of ceramic materials and components, Part 2: Methods of measurement – Low po*wer*, CENELEC European Committee for Electrotechnical Standardization, 2002.

[22] J.E. Kogel, N.C. Trivedi, J. M. Barker, S.T.Krukowski , Industrial Minerals & Rocks: Commodities, Markets, and Uses, 7th EDITION, Society for mining, metallurgy and Exploration Inc. (SME), 2006, pag. 1193-1203, ISBN-13 978-0-87335-233-8.

[23] O. Bortnovsky, J. Dedeček, Z. Tvarůžková, Z. Sobalík, J. Šubrt, Metal ions as probes for characterization of geopolymer materials, J. Am. Ceram. Soc., 2008, 91 3052–3057.

[24] W.M. Kriven, J.L. Bell, M. Gordon, Microstructure and microchemistry of fully reacted geopolymer and geopolymer composites, Ceramic Transactions 2003, 153, 227-250.

[25] P. Sazamaa, O. Bortnovsky, J. Dedecek, Z. Tvaruzková, Z. Sobalík, Geopolymer based catalysts—New group of catalytic materials, Catalysis Today, 2011, 164, 92–99.

[26] P. Duxson, John L. Provis, Grant C. Lukey, Frances Separovic, Jannie S. J. van Deventer, ^{29}Si NMR Study of Structural Ordering in Aluminosilicate Geopolymer Gels Langmuir 2005, 21, 3028-3036.

[27] P. Duxson, G. C. Lukey, F. Separovic, J. S. J. van Deventer**,** Effect of Alkali Cations on Aluminum Incorporation in Geopolymeric Gels Ind. Eng. Chem. Res. 2005, 44, 832-839.

[28] D. W. Breck, Zeolite Molecular Sieves, Krieger, Malabar, 1984.

[29] A. R. Ruiz-Salvador, D. W. Lewis, J. Rubayo-Soneira, G. Rodriguez-Fuentes, L. R. Sierra, C. R. A. Catlow**,** Aluminum distribution in low Si/Al zeolites: Dehydrated Na-clinoptilolite J. Phys. Chem. *B* 1998, 102 (43), 8417–8425.

[30] D.Seoung, Y.Lee, C.-C. Kao, T. Vogt, Y. Lee, Super-hydrated zeolites: pressure-induced hydration in natrolites, Chem. Eur. J. 2013, 19, 10876 – 10883

[A] Y. Elakneswaran, T. Nawa, K. Kurumisawa, Electrokinetic potential of hydrated cement in relation to adsorption of chlorides, Cement and Concrete Research, 2009, 39 340–344.

[32] Y. Lee, J. A. Hriljac, T. Vogt, J. B. Parise, G. Artioli, First Structural Investigation of a Super-Hydrated Zeolite J. Am. Chem. Soc. 2001, 123, 12732–12733**.**

[33] Y. Lee, T. Vogt, J. A. Hriljac, J. B. Parise, J. C. Hanson, S. J. Kim, Non-framework cation migration and irreversible pressure-induced hydration in a zeolite Nature 2002, 420, 485–489.

[34] Toledo, P. G., H. T. Davis, and L. E. Scriven, Transport properties of anisotropic porous media: Effective medium theory, Chem. Eng. Sci. 1992, 47, 391–405.

[35] S.P. Friedman, S. B. Jones, Measurement and approximate critical path analysis of the pore-scale-induced anisotropy factor of an unsaturated porous medium, Water Resources Research 2001, 37-12, 2929–2942.

[36] L.R. Van Loon, J. Soier, W. Muller, M.H. Bradbury, Anisotropic diffusion in layered argillaceous rocks: a case study with opalinus clay, PSI- Scientific Report 2002 / Volume IV Nuclear Energy and Safety, 97-104, ISSN 1423-7334.

[37] M. Cieszko, Description of anisotropic pore space structure of permeable materials based on Minkowski metric space, Arch. Mech., 61, 6, pp. 425–444, Warszawa 2009

[38] F.-J. Ulm, G. Constantinides and F. H. Heukamp, Is concrete a poromechanics materials?—A multiscale investigation of poroelastic properties, Materials and Structres / Concrete Science and Engineering 2004, 37, 43-58.

[39] T. Rougelot F. Skoczylas, N.Burlion, Water desorption and shrinkage in mortars and cement pastes: Experimental study and poromechanical model, Cement and Concrete Research 2009, 39, 36–44.

[40] F. Skoczylas, N.Burlion, I. Yurtdas, About drying effects and poro-mechanical behaviour of mortars, Cement and Concrete composite 2007, 29, 383-390.

[41] J. H.m. Visser, Extensile Hydraulic fracturing of (saturated) porous materials ISBN 90- 407-1699-4/CIP

[42] J.M. Torrenti, G. Pijaudier-Cabot, J. M. Reynouard Behavior of Concrete, ISBN 978-1-84821-178-0